To summarize, the performances of LS and SR-LS differ in general. The simulations and discussion here suggest that the worst-case performance ratio $\sqrt{\Delta}$ can be larger if the ranges $d_1, \ldots, d_M$ span a large range. While we believe that the examples and discussion here give substantial insight, we must state the complete characterization of bad geometries for SR-LS as an open problem.

VI. Conclusion

Compared to classical LS, SR-LS [1] is a computationally very attractive approach to the source localization problem, since it can find the global minimum of the cost function without resorting to heuristic divide-and-conquer methods or heuristic techniques for solving nonconvex optimization problems. We have computed and compared the asymptotic accuracies of LS and SR-LS. Our main observations are i) there exist geometries, where LS and SR-LS have identical performances and ii) there are geometries, for which the difference in performance between LS and SR-LS is unbounded. We also exemplified the asymptotic performance difference numerically for random geometries. Taken together, SR-LS performs well relative to LS for most geometries, but not for all. If SR-LS is used in practice, then care should be taken to avoid the geometries that the method has difficulties with. If the position of $\mathcal{S}$ is approximately known *a priori*, then the achievable accuracy can be estimated by using (14) and (19), before choosing what localization algorithm to use.

The numerical results presented in this paper are reproducible. To obtain the relevant MATLAB programs go to www.commsys.isy.liu.se/~egl/rr . Included therein is also Monte Carlo simulation code for numerically verifying the validity of the asymptotic accuracy formulas that we derived.

References

[1] A. Beck, P. Stoica, and J. Li, "Exact and approximate solutions of source localization problems," *IEEE Trans. Signal Process.*, vol. 56, no. 5, pp. 1770–1778, May 2008.

[2] *Global Positioning System: Theory and Applications*, ser. Progress in Astronautics and Aeronautics, B. Parkinson and J. Spilker, Jr., Eds. Washington, DC: Amer. Instit. Aeronautics Astronautics, 1996, vol. 163.

[3] J. Caffery, Jr. and G. Stüber, "Subscriber location in CDMA cellular networks," *IEEE Trans. Veh. Technol.*, vol. 47, pp. 406–416, May 1998.

[4] G. Sun, J. Chen, W. Guo, and K. Liu, "Signal processing techniques in network-aided positioning: A survey of state-of-the-art positioning designs," *IEEE Signal Process. Mag.*, vol. 22, no. 4, pp. 12–23, Jul. 2005.

[5] K.-F. Ssu, C.-H. Ou, and H. Jiau, "Localization with mobile anchor points in wireless sensor networks," *IEEE Trans. Veh. Technol.*, vol. 54, pp. 1187–1197, May 2005.

[6] S. M. Kay, *Fundamentals of Statistical Signal Processing: Estimation Theory*. Englewood Cliffs, NJ: Prentice-Hall, 1993.

[7] K. Cheung, H. So, W.-K. Ma, and Y. Chan, "Least squares algorithms for time-of-arrival-based mobile location," *IEEE Trans. Signal Process.*, vol. 52, no. 4, pp. 1121–1130, Apr. 2004.

[8] L. Ljung, *System Identification: Theory for the User*, 2nd ed. Englewood Cliffs, NJ: Prentice-Hall, 1998.

[9] M. Viberg and B. Ottersten, "Sensor array processing based on subspace fitting," *IEEE Trans. Signal Process.*, vol. 39, no. 5, pp. 1110–1121, May 1991.

[10] P. Stoica and T. Söderström, *System Identification*. Englewood Cliffs, NJ: Prentice-Hall, 1989.

[11] A. Papoulis, *Probability, Random Variables, and Stochastic Processes*, 3rd ed. New York: McGraw-Hill, 1991.

Efficient Estimation of a Narrow-Band Polynomial Phase Signal Impinging on a Sensor Array

Alon Amar

***Abstract*—The parameters of interest of a polynomial phase signal observed by a sensor array include the direction of arrival and the polynomial coefficients. The direct maximum likelihood estimation of these parameters requires a nonlinear multidimensional search. In this paper, we present a two-step estimation approach. The estimation requires only a one-dimensional search in the direction of arrival space and involves a simple least squares solution for the polynomial coefficients. The efficiency of the estimates is corroborated by Monte Carlo simulations.**

***Index Terms*—Extended invariance property, maximum likelihood estimation, polynomial phase signal.**

I. Introduction

Polynomial phase signals (PPSs) attract attention in radar, sonar, and communications systems. Previous research has considered PPSs observed with a single sensor [1]–[5] and also with a sensor array [6]–[10]. We focus on the latter case here. The parameters of interest are the direction of arrival (DOA) and the polynomial coefficients of the signal's phase.

The maximum likelihood estimator (MLE) requires a large amount of computation since it involves the maximization of a multivariable cost function and is therefore not practically useful. For example, the MLE in [6] extracts the parameters of a chirp signal (PPS of order two) with a three-dimensional search in the DOA, frequency, and frequency-rate spaces.

The goal of this paper is to suggest an efficient parameter estimation of a single narrow-band PPS impinging on an array, based on the extended invariance property (EXIP) [11]. It is shown that the DOA is estimated by a one-dimensional search and that the polynomial coefficients are obtained by a simple least squares (LS) solution. Simulation results corroborate that the estimates asymptotically converge to the Cramér–Rao lower bound (CRLB) at high signal-to-noise ratio (SNR).

II. Problem Formulation

Consider a uniform linear array (ULA) composed of M sensors. Assume that the transmitted signal can be modeled as $\tilde{s}(t;\alpha,\mathbf{b}) \triangleq \alpha e^{j\tilde{\phi}(t;\mathbf{b})}$, where α is the unknown amplitude, $\tilde{\phi}(t;\mathbf{b}) = \omega_0 t + \phi(t;\mathbf{b})$, where ω_0 is the carrier frequency, and $\phi(t;\mathbf{b}) \triangleq \mathbf{b}^T\mathbf{u}(t)$ with $\mathbf{u}(t) \triangleq [1, t, \ldots, t^P]^T$, P is the known polynomial order, and $\mathbf{b} \triangleq [b_0, b_1, \ldots, b_P]^T$ is the vector of polynomial coefficients. The noiseless signal observed at the mth element of the array over the time interval $T_0 \le t \le T_0 + T$ is $\tilde{x}_m(t) = (\alpha/\sqrt{M})e^{j\tilde{\phi}(t+\tau_m;\mathbf{b})}$, $m = 1, \ldots, M$, where $\tau_m = (d/c)(m-1)\sin(\theta)$, θ is the signal's DOA, c is the propagation speed of the signal, and d is the interelement spacing. According to the mean value theorem of Lagrange, we can write

Manuscript received March 08, 2009; accepted July 17, 2009. First published August 18, 2009; current version published January 13, 2010. The associate editor coordinating the review of this manuscript and approving it for publication was Prof. Antonio Napolitano. This work was supported in part by NWO-STW under the VICI program (DTC.5893).

The author is with the Circuits and Systems Group, Faculty of Electrical Engineering, Mathematics and Computer Science, Delft University of Technology, Delft 2628 CD, The Netherlands (e-mail: a.amar@tudelft.nl).

Digital Object Identifier 10.1109/TSP.2009.2030608

$\tilde{\phi}(t+\tau_m;\mathbf{b}) = \tilde{\phi}(t;\mathbf{b}) + (d/dt)\tilde{\phi}(t_m;\mathbf{b})\tau_m$, where $t \le t_m \le t+\tau_m$ [8, p. 342]. The noiseless vector of the received signals at the array output can then be written as $\tilde{\mathbf{x}}(t) = \tilde{\mathbf{a}}(t;\theta,\mathbf{b})\tilde{s}(t;\alpha,\mathbf{b})$, where $\tilde{\mathbf{x}}(t) \triangleq [\tilde{x}_1(t),\ldots,\tilde{x}_M(t)]^T$, $\tilde{\mathbf{a}}(t;\theta,\mathbf{b}) \triangleq (1/\sqrt{M})[1, e^{j\omega_0(1+\eta(t_2))\tau_2(\theta)},\ldots,e^{j\omega_0(1+\eta(t_M))\tau_M(\theta)}]^T$, and $\eta(t_m) \triangleq (1/\omega_0)(d\phi(t_m;\mathbf{b})/dt)$ represents the deviation of the signal frequency around the carrier frequency. Let W denote the bandwidth of the signal. We consider the case of a narrow-band signal, that is, $\max_m \eta(t_m) \le (W/\omega_0) \ll 1$. In this case, $\tilde{\mathbf{a}}(t;\theta,\mathbf{b}) \cong \mathbf{a}(\theta)$, where $\mathbf{a}(\theta) = (1/\sqrt{M})[1,\ldots,e^{j(\omega_0/c)d(M-1)\sin\theta}]^T$. Let $\mathbf{x}(n) = \tilde{\mathbf{x}}(n)e^{-j\omega_0 t}$ be the array outputs after down-conversion to baseband. We then sample $\mathbf{x}(t)$ with a sampling interval denoted by Δ. The vector containing the noisy received signals is [8]–[10]

$$\mathbf{x}(n) = \mathbf{a}(\theta)s(n;\alpha,\mathbf{b}) + \mathbf{e}(n), \quad n = n_0,\ldots,n_0+N-1 \tag{1}$$

where $N = \lfloor T/\Delta \rfloor$ is the number of samples, $n_0 = \lfloor T_0/\Delta \rfloor$, $s(n;\alpha,\mathbf{b}) \triangleq \alpha e^{j\mathbf{b}^T\mathbf{u}(n\Delta)}$, and $\mathbf{e}(n)$ is the $M\times 1$ noise vector assumed to be a spatially and temporally white Gaussian complex random vector with zero mean and covariance matrix $\sigma^2\mathbf{I}_M$, where $\mathbf{I}_M$ is the $M \times M$ identity matrix.

The problem discussed herein is as follows. Given the observations $\{\mathbf{x}(n)\}_{n=n_0}^{n_0+N-1}$, estimate the parameter vector $\boldsymbol{\psi} \triangleq [\mathbf{b}^T,\theta,\alpha,\sigma^2]^T$, where $\mathbf{b}$ and θ are the parameters of interest while α and σ^2 are nuisance parameters.

III. Maximum Likelihood Estimator

The maximum likelihood (ML) technique directly estimates $\boldsymbol{\psi}$ from the given observations as follows. The negative log-likelihood function (LLF) is

$$L(\boldsymbol{\psi}) = MN\ln\sigma^2 + \frac{1}{\sigma^2}\sum_{n=n_0}^{n_0+N-1}\left\|\mathbf{x}(n) - \alpha\mathbf{a}(\theta)e^{j\mathbf{b}^T\mathbf{u}(n\Delta)}\right\|^2 \tag{2}$$

Differentiating (2) with respect to σ^2 and equating the result to zero yields that the MLE of σ^2 is $\hat{\sigma}^2 = (1/MN)\sum_{n=n_0}^{n_0+N-1}\|\mathbf{x}(n) - \hat{\alpha}\mathbf{a}(\hat{\theta})e^{j\hat{\mathbf{b}}^T\mathbf{u}(n\Delta)}\|^2$. Inserting $\hat{\sigma}^2$ into (2) yields that $\{\hat{\alpha},\hat{\theta},\hat{\mathbf{b}}\}$ maximize

$$L_1(\alpha,\theta,\mathbf{b}) = 2\alpha\Re\left\{e^{-jb_0}\mathbf{a}^H(\hat{\theta}) \times \sum_{n=n_0}^{n_0+N-1} e^{-j\sum_{p=1}^{P} b_p(n\Delta)^p}\mathbf{x}(n)\right\} - \alpha^2 N. \tag{3}$$

Define by $\beta \triangleq (1/N)\sum_{n=n_0}^{n_0+N-1}\mathbf{a}^H(\hat{\theta})\mathbf{x}(n)e^{-j\sum_{p=1}^{P}\hat{b}_p(n\Delta)^p}$. The estimates of b_0 and α are then $\hat{b}_0 = \arg\{\beta\}$ and $\hat{\alpha} = |\beta|$, where $\arg(x) \in [0,2\pi)$ is the phase of x. Finally, substituting $\hat{b}_0$ and $\hat{\alpha}$ into (3) yields

$$\left\{\{\hat{b}_p\}_{p=1}^{P},\hat{\theta}\right\} = \arg\max_{\{b_p\}_{p=1}^{P},\theta}\left|\sum_{n=n_0}^{n_0+N-1}\mathbf{a}^H(\theta)\mathbf{x}(n)e^{-j\sum_{p=1}^{P}b_p(n\Delta)^p}\right|^2. \tag{4}$$

Given the above estimates, we define the vector of the (direct) ML estimated parameters as $\hat{\boldsymbol{\psi}} \triangleq [\hat{\mathbf{b}}^T,\hat{\theta},\hat{\alpha},\hat{\sigma}^2]^T$. The result in (4) is the narrow-band version of the result in [6, (53)]. This estimation requires a large amount of computation since it involves the maximization of a multivariable cost function.

We estimate the complexity of the MLE based on the number of multiplication operations. Let N_θ and N_b be the number of grid points in the spaces of θ and $\mathbf{b}$, respectively. The complexity of the cost function in (4) is $N_\theta N_b^P N(M+P+1)$. Similarly, the complexities of computing $\hat{b}_0$ and $\hat{\alpha}$ are $N(M+P+1)$, and that of $\hat{\sigma}^2$ is $N(2M+P+1)$. The overall complexity is $N[(N_\theta N_b^P+3)(M+P+1)+M] \cong N_\theta N_b^P N(M+P+1)$, which increases exponentially with the order of the polynomial.

IV. Cramér–Rao Lower Bound

We derive explicit expressions for the CRLB on the accuracy of estimating $\boldsymbol{\psi}$. The Fisher information matrix (FIM) on the estimation of $\boldsymbol{\psi}$ is given by $\mathbf{J} \triangleq E\{\partial^2 L(\boldsymbol{\psi})/\partial\boldsymbol{\psi}\partial\boldsymbol{\psi}^T\}$. Using the closed-form expressions as given in [13, (8.33)], it can be shown that

$$\mathbf{J} = \begin{bmatrix} \frac{2\alpha^2}{\sigma^2}\mathbf{U}\mathbf{U}^T & \frac{2c_1\alpha^2}{\sigma^2}\cos(\theta)\mathbf{U}\mathbf{1}_N & \mathbf{0}_N & \mathbf{0}_N \\ \frac{2c_1\alpha^2}{\sigma^2}\cos(\theta)\mathbf{1}_N^T\mathbf{U}^T & \frac{2Nc_2\alpha^2}{\sigma^2}\cos^2(\theta) & 0 & 0 \\ \mathbf{0}_N^T & 0 & \frac{2N}{\sigma^2} & 0 \\ \mathbf{0}_N^T & 0 & 0 & \frac{NM}{\sigma^4} \end{bmatrix} \tag{5}$$

where $\mathbf{1}_N$ is an $N\times 1$ vectors with all elements equal to one, $\mathbf{0}_N$ is an $N\times 1$ vector with all elements equal to zero, and where we defined the $(P+1) \times N$ Vandermonde matrix

$$\mathbf{U} \triangleq [\mathbf{u}(n_0\Delta),\ldots,\mathbf{u}((n_0+N-1)\Delta)] \tag{6}$$

and also

$$c_1 \triangleq \frac{d\omega_0}{c}\kappa_1, \quad c_2 \triangleq \left(\frac{d\omega_0}{c}\right)^2\kappa_2 \tag{7}$$

$$\kappa_1 \triangleq \frac{1}{2}(M-1), \quad \kappa_2 \triangleq \frac{1}{6}(M-1)(2M-1). \tag{8}$$

Using the matrix inversion formula [13, (A.68)], the CRLB matrix, denoted by $\boldsymbol{\Gamma}(\boldsymbol{\psi}) \triangleq \mathbf{J}^{-1}$, is

$$\boldsymbol{\Gamma}(\boldsymbol{\psi}) = \begin{bmatrix} \frac{\sigma^2}{2\alpha^2}\mathbf{P} & -\frac{\sigma^2}{2\alpha^2}\mathbf{z} & \mathbf{0}_N & \mathbf{0}_N \\ -\frac{\sigma^2}{2\alpha^2}\mathbf{z}^T & \frac{\sigma^2}{2\alpha^2}\frac{1}{Nc_2\mu\cos^2(\theta)} & 0 & 0 \\ \mathbf{0}_N^T & 0 & \frac{\sigma^2}{2N} & 0 \\ \mathbf{0}_N^T & 0 & 0 & \frac{\sigma^4}{NM} \end{bmatrix} \tag{9}$$

where

$$\mathbf{P} \triangleq (\mathbf{U}\mathbf{U}^T)^{-1} + \frac{\kappa_1^2}{N\kappa_2\mu}\mathbf{U}^+\mathbf{1}_N\mathbf{1}_N^T(\mathbf{U}^+)^T \tag{10}$$

$$\mathbf{z} \triangleq \frac{c_1}{Nc_2\mu\cos(\theta)}\mathbf{U}^+\mathbf{1}_N \tag{11}$$

$$\mu \triangleq 1 - \frac{\kappa_1^2}{N\kappa_2}\mathbf{1}_N^T\mathbf{U}^T\mathbf{U}^+\mathbf{1}_N \tag{12}$$

and $\mathbf{U}^+ \triangleq (\mathbf{U}\mathbf{U}^T)^{-1}\mathbf{U}$. It is easy to verify that for $P = 1, 2$, we get $\mathbf{1}_N^T\mathbf{U}^T\mathbf{U}^+\mathbf{1}_N = N$, and that $\mathbf{U}^+\mathbf{1}_N = \mathbf{e}_1$, where $\mathbf{e}_1$ is the first column of $\mathbf{I}_{P+1}$. For larger values of P, using numerical software tools, it can be verified that these results still hold. Therefore, we obtain that $\mu = 1 - (\kappa_1^2/\kappa_2)$. Using these results, we can rewrite $\boldsymbol{\Gamma}(\boldsymbol{\psi})$ also as

$$\boldsymbol{\Gamma}(\boldsymbol{\psi}) = \begin{bmatrix} \frac{\sigma^2}{2\alpha^2}\tilde{\mathbf{P}} & -\frac{\sigma^2}{2\alpha^2}\tilde{\mathbf{z}} & \mathbf{0}_N & \mathbf{0}_N \\ -\frac{\sigma^2}{2\alpha^2}\tilde{\mathbf{z}}^T & \frac{\sigma^2}{2\alpha^2}\frac{1}{Nc_2\mu\cos^2(\theta)} & 0 & 0 \\ \mathbf{0}_N^T & 0 & \frac{\sigma^2}{2N} & 0 \\ \mathbf{0}_N^T & 0 & 0 & \frac{\sigma^4}{NM} \end{bmatrix} \tag{13}$$

where

$$\tilde{\mathbf{P}} \triangleq (\mathbf{U}\mathbf{U}^T)^{-1} + \frac{\kappa_1^2}{N\kappa_2\mu}\mathbf{e}_1\mathbf{e}_1^T \tag{14}$$

$$\tilde{\mathbf{z}} \triangleq \frac{c_1}{Nc_2\mu\cos(\theta)}\mathbf{e}_1. \tag{15}$$

For a large number of elements in the array, that is, $M \gg 1$, we get that $(\kappa_1^2/\kappa_2) \cong (3/4)$, and thus, $\mu \cong (1/4)$. Observe that the CRLB on the DOA is identical with the CRLB derived in [12, p. 3127] for the case of a single constant modulus signal. Also, the cross-term between the DOA and the polynomial parameters approaches zero as N increases, and therefore their estimation is decoupled. This can also be seen from the CRLB on $\mathbf{b}$, which does not depend on the array parameters as N increases, since the last term of this CRLB approaches zero as N increases.

V. Proposed Two-Step Estimator

The major difficulty of the direct MLE of $\boldsymbol{\psi}$ is that it requires a multidimensional search. Instead, we estimate $\boldsymbol{\psi}$ with a two-step approach using the EXIP [11], which substantially reduces the computation load. The two-step approach was mentioned also in [2] and [5] but for a single sensor and without using the EXIP.

Consider the negative LLF in (2). We reparameterize it by a vector of intermediate parameters $\boldsymbol{\psi}_i$, such that $L(\boldsymbol{\psi}_i)$ is equivalent to $L(\boldsymbol{\psi})$, where $\boldsymbol{\psi}_i \triangleq [\boldsymbol{\phi}^T, \theta_i, \alpha_i, \sigma_i^2]^T$ with $\boldsymbol{\phi} \triangleq [\phi(1), \ldots, \phi(N)]^T$, and $\phi(n) \triangleq \mathbf{b}^T\mathbf{u}(n\Delta)$ represents the instantaneous phase. We thus have the following one-to-one mapping:

$$\boldsymbol{\psi}_i = \mathbf{F}\boldsymbol{\psi} \tag{16}$$

where $\mathbf{F}$ is the $(N+3)\times(P+4)$ matrix defined as

$$\mathbf{F} \triangleq \begin{bmatrix} \mathbf{U}^T & \mathbf{O}_{N\times 3} \\ \mathbf{O}_{3\times(P+1)} & \mathbf{I}_3 \end{bmatrix} \tag{17}$$

and $\mathbf{O}_{n\times m}$ is an $n\times m$ matrix with all elements equal to zero. Notice that the mapping from θ, α, σ^2 to $\theta_i, \alpha_i, \sigma_i^2$ is one-to-one. Moreover, given the time samples $\{n\Delta\}_{n=n_0}^{n_0+N-1}$, assume that there exists another vector $\mathbf{b}'$ such that $\boldsymbol{\phi} = \mathbf{U}^T\mathbf{b} = \mathbf{U}^T\mathbf{b}'$, that is, $\mathbf{U}^T(\mathbf{b}-\mathbf{b}') = \mathbf{0}$. Since $\mathbf{U}^T$ is a full column rank Vandermonde matrix, then $\mathbf{b} = \mathbf{b}'$, and thus $\boldsymbol{\phi} = \mathbf{U}^T\mathbf{b}$ is also a one-to-one mapping.

According to the EXIP, we estimate $\boldsymbol{\psi}$ with two subsequent steps: 1) estimate $\boldsymbol{\psi}_i$ and 2) estimate $\boldsymbol{\psi}$ given the previous results using the appropriate weighted least squares (WLS) approach.

A. Estimating the Vector of Intermediate Parameters $\boldsymbol{\psi}_i$

Denote the ML estimated vector of $\boldsymbol{\psi}_i$ by $\hat{\boldsymbol{\psi}}_i \triangleq [\hat{\boldsymbol{\phi}}^T, \hat{\theta}_i, \hat{\alpha}_i, \hat{\sigma}_i^2]^T$, where the estimated vector of $\boldsymbol{\phi}$ is $\hat{\boldsymbol{\phi}} = [\hat{\phi}(1), \ldots, \hat{\phi}(N)]^T$. The vector $\hat{\boldsymbol{\psi}}_i$ is the minimizer of the negative LLF parameterized by $\boldsymbol{\psi}_i$

$$L(\boldsymbol{\psi}_i) = MN\ln\sigma_i^2 + \frac{1}{\sigma_i^2}\sum_{n=n_0}^{n_0+N-1}\left\|\mathbf{x}(n) - \alpha_i\mathbf{a}(\theta_i)e^{j\phi(n)}\right\|^2. \tag{18}$$

Differentiating (18) with respect to σ_i^2 and equating the result to zero yields that the MLE of σ_i^2 is $\hat{\sigma}_i^2 = (1/MN)\sum_{n=n_0}^{n_0+N-1}\|\mathbf{x}(n) - \hat{\alpha}_i\mathbf{a}(\hat{\theta}_i)e^{j\hat{\phi}(n)}\|^2$. Substituting $\hat{\sigma}_i^2$ in (18) yields that $\hat{\alpha}_i, \hat{\theta}_i, \hat{\phi}(n)$ minimize

$$L_1(\alpha_i, \theta_i, \phi(n)) = \alpha^2 - \frac{2\alpha}{N} \times \sum_{n=n_0}^{n_0+N-1}\left|\mathbf{a}^H(\theta)\mathbf{x}(n)\right|\cos\left(\arg\left(\mathbf{a}^H(\theta)\mathbf{x}(n)\right) - \phi(n)\right). \tag{19}$$

It is clear from (19) that $\hat{\phi}(n) = \arg(\mathbf{a}^H(\hat{\theta}_i)\mathbf{x}(n))$ and $\hat{\alpha}_i = (1/N)\sum_{n=n_0}^{n_0+N-1}|\mathbf{a}^H(\hat{\theta}_i)\mathbf{x}(n)|$. By substituting $\hat{\phi}(n)$ and $\hat{\alpha}_i$ into (19), we obtain that the MLE of θ_i is

$$\hat{\theta}_i = \arg\max_{\theta}\sum_{n=n_0}^{n_0+N-1}\left|\mathbf{a}^H(\theta)\mathbf{x}(n)\right|. \tag{20}$$

The phases $\hat{\phi}(n)$ are obtained by substituting (20) into $\hat{\phi}(n)$. Note that it is required to perform phase unwrapping on $\{\mathbf{a}^H(\hat{\theta}_i)\mathbf{x}(n)\}_{n=n_0}^{n_0+N-1}$ in order to have a continuous phase, instead of a discontinuous phase defined in $[0, 2\pi)$. We adopt the phase unwrapping procedure presented in [2, p. 2119]. The unwrapped phases of $\{\mathbf{a}^H(\hat{\theta}_i)\mathbf{x}(n)\}_{n=n_0}^{n_0+N-1}$ are

$$\begin{aligned}
\hat{\phi}(n_0) &= \arg\left(\mathbf{a}^H(\hat{\theta}_i)\mathbf{x}(n_0)\right) \\
\hat{\phi}(n_0+1) &= \arg\left(\mathbf{a}^H(\hat{\theta}_i)\mathbf{x}(n_0+1)\left(\mathbf{a}^H(\hat{\theta}_i)\mathbf{x}(n_0)\right)^*\right) \\
&\quad + \hat{\phi}(n_0) \\
\hat{\phi}(n) &= \Delta^2\hat{\phi}(n) + 2\hat{\phi}(n-1) - \hat{\phi}(n-2), \\
&\quad n = n_0+2, \ldots, n_0+N-1
\end{aligned} \tag{21}$$

where

$$\Delta^2\hat{\phi}(n) \triangleq \arg\left(\mathbf{a}^H(\hat{\theta}_i)\mathbf{x}(n)\left(\mathbf{a}^H(\hat{\theta}_i)\mathbf{x}(n-1)\right)^* \times \left(\mathbf{a}^H(\hat{\theta}_i)\mathbf{x}(n-1)\right)^*\mathbf{a}^H(\hat{\theta}_i)\mathbf{x}(n-2)\right). \tag{22}$$

B. Estimating $\boldsymbol{\psi}$ Using WLS

Denote the indirect estimate of $\boldsymbol{\psi}$ as $\hat{\boldsymbol{\psi}}' \triangleq [\hat{\mathbf{b}}'^T, \hat{\theta}', \hat{\alpha}', \hat{\sigma}^{2\prime}]^T$. According to the EXIP, $\hat{\boldsymbol{\psi}}'$ is given as [11]

$$\hat{\boldsymbol{\psi}}' = \arg\min_{\boldsymbol{\psi}}[\hat{\boldsymbol{\psi}}_i - \mathbf{F}\boldsymbol{\psi}]^T\mathbf{W}[\hat{\boldsymbol{\psi}}_i - \mathbf{F}\boldsymbol{\psi}] = (\mathbf{F}^T\mathbf{W}\mathbf{F})^{-1}\mathbf{F}^T\mathbf{W}\hat{\boldsymbol{\psi}}_i \tag{23}$$

where $\mathbf{W} \triangleq E\{\partial^2 L(\boldsymbol{\psi}_i)/\partial\boldsymbol{\psi}_i\partial\boldsymbol{\psi}_i^T\}|_{\boldsymbol{\psi}_i=\hat{\boldsymbol{\psi}}_i}$ is the $(N+3)\times(N+3)$ FIM on the estimation of $\boldsymbol{\psi}_i$ evaluated at $\hat{\boldsymbol{\psi}}_i$. Similarly to Section IV, using the result in [13, (8.33)], it can be shown that

$$\mathbf{W} = \begin{bmatrix} \frac{2\hat{\alpha}_i^2}{\sigma^2}\mathbf{I}_N & \frac{2c_1\hat{\alpha}_i^2}{\sigma^2}\cos(\hat{\theta}_i)\mathbf{1}_N & \mathbf{0}_N & \mathbf{0}_N \\ \frac{2c_1\hat{\alpha}_i^2}{\sigma^2}\cos(\hat{\theta}_i)\mathbf{1}_N^T & \frac{2Nc_2\hat{\alpha}_i^2}{\sigma^2}\cos^2(\hat{\theta}_i) & 0 & 0 \\ \mathbf{0}_N^T & 0 & \frac{2N}{\sigma^2} & 0 \\ \mathbf{0}_N^T & 0 & 0 & \frac{NM}{\sigma^4} \end{bmatrix}. \tag{24}$$

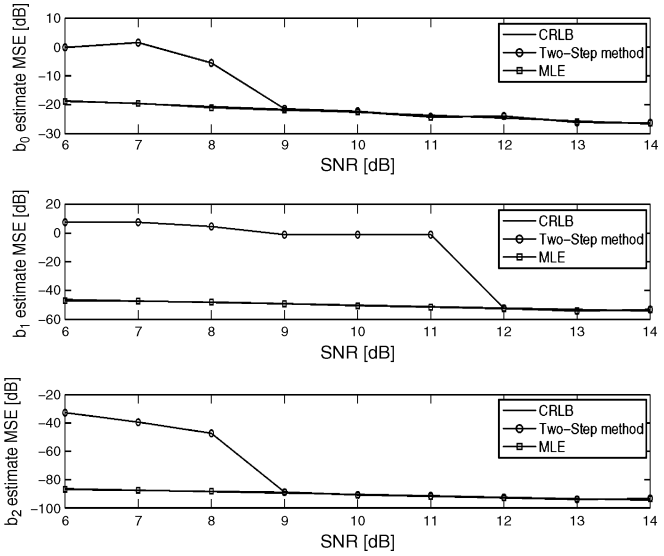

Fig. 1. MSEs of the estimated $\{b_p\}_{p=0}^2$ using the proposed method and the MLE, and their associated CRLBs, versus the SNR.

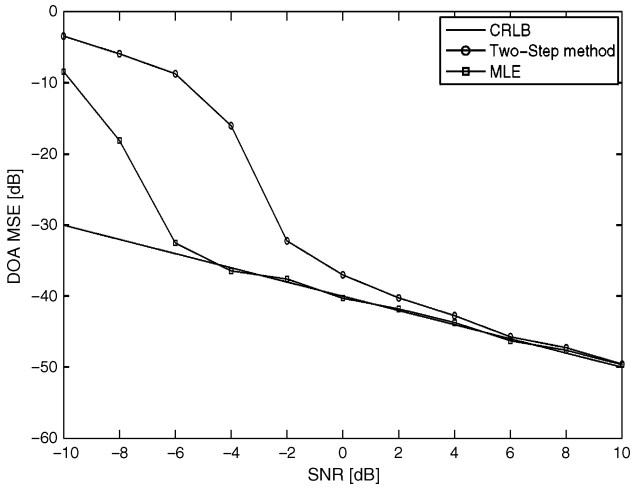

Fig. 2. MSEs of the estimated DOA using the proposed method and the MLE, and the associated CRLB, versus the SNR.

Combining (17) and (24) with (23), we obtain that the estimates using the EXIP are

$$\mathbf{b}' = \left[\mathbf{U}^+ + \frac{\kappa_1^2}{N\kappa_2\mu}\mathbf{e}_1\mathbf{1}_N^T\left(\mathbf{U}^T(\mathbf{U}\mathbf{U}^T)^{-1}\mathbf{U} - \mathbf{I}\right)\right]\hat{\boldsymbol{\phi}}$$
$$\hat{\theta}' = \hat{\theta}_i,\ \hat{\alpha}' = \hat{\alpha}_i,\ \hat{\sigma}^{2\prime} = \hat{\sigma}_i^2. \tag{25}$$

Notice that although theoretically the weighting matrix $\mathbf{W}$ is evaluated at the values of the estimates of the first estimation step, in this case, the matrix multiplying $\hat{\boldsymbol{\phi}}$ can be evaluated offline. Also, if N is large enough, then $\mathbf{b}' = \mathbf{U}^+\hat{\boldsymbol{\phi}}$, which is the LS solution of $\mathbf{b}'$ given the vector of estimates $\hat{\boldsymbol{\phi}}$.

We estimate the computational complexity of the proposed method. Since the matrix multiplying $\hat{\boldsymbol{\phi}}$ can be evaluated offline, its computation will not be taken into account. The complexity of $\hat{\phi}(n)$, $\hat{\alpha}_i$, and σ_i^2 are M, NM, and $2NM$, respectively. The complexity of (20) is $N_\theta NM$, where N_θ is the number of grid points in the space of θ. The complexity of the unwrapping step is approximately on the order of NM. Therefore, the overall complexity is $N_\theta NM + 4NM + M$, which is on the order of $N_\theta NM$. Clearly, the complexity of the proposed method is less than the complexity of the MLE.

VI. Numerical Examples

We present the results of several simulated experiments. In the first three simulations, we consider a chirp signal given by [8] $s(n;\alpha,\mathbf{b}) = e^{j((\pi/4)-(2\pi 0.4/\Delta)((n\Delta)-(n\Delta)^2/N))}$, where $\Delta = 1$, $n_0 = 0$, and $N = 100$. We use an eight-element ULA with half-wavelength spacing ($d = \pi c/\omega_0$). The signal's DOA is 10°. The noise power σ^2 is adjusted to give the desired SNR, defined by SNR$= -10\log_{10}\sigma^2$ [dB].

In the first simulation, we compare the mean square error (MSE) of the estimates of b_0, b_1, and b_2 of the direct MLE and the proposed method versus the SNR. We consider SNR values from 6 [dB] to 14 [dB] with a step of 1 [dB]. At each SNR, we evaluated the MSE of b_p with $N_{exp} = 100$ Monte Carlo (MC) independent trials. The results are presented in Fig. 1. We also plotted the associated CRLB of b_0, b_1, and b_2. As can be seen, the estimates approach the CRLB for sufficiently high SNR. However, for low SNR, the performance of the MLE is superior.

In the second simulation, we compared the MSE of the estimated DOA of the MLE and the proposed method versus the SNR. The SNR was varied from -10 to 10 [dB] with a step of 2 [dB]. At each SNR, we evaluated the MSE of the DOA with $N_{\exp} = 100$ MC independent trials. The results are presented in Fig. 2. We also plotted the associated CRLB of the DOA. As can be seen, the DOA estimates approach the CRLB for sufficiently high SNR, while the ML estimate is superior for low SNR.

In the third simulation, we corroborated the narrow-band assumption leading to (1). We examined the MSEs of the MLE and the proposed method (both derived using the narrow-band assumption) given data generated according to the wide-band signal model, as detailed in Section II. As in [8, p. 345] we used a frequency sampling of $1/\Delta = 8192$[Hz]. Also $N = 100$, and SNR $= 15$ [dB]. Notice that the (continuous) signal occupies the bandwidth $[-0.4/\Delta, 0.4/\Delta]$ around the carrier frequency ω_0, where $1/2\Delta$ is the aliasing free bandwidth of the signal. Recall that (1) was obtained under the assumption that $W/\omega_0 \ll 1$. We therefore varied ω_0 from $10^2 \times (1/2\Delta)$ to $10^4 \times (1/2\Delta)$ with a step of $5 \times 10^2 \times (1/2\Delta)$. At each value of ω_0, we calculated the MSE of b_p for the MLE and the proposed method, with $N_{\exp} = 100$ MC independent trials. The results are presented in Fig. 3. We also plotted the CRLB of b_0, b_1, and b_2 (calculated using the narrow-band assumption). As can be seen up to a ratio of 0.005 (associated with $\omega_0 = 0.8192$ [MHz]), the MSEs of all the estimates agree with the CRLB. Moreover, even at a ratio of 0.01 (associated with $\omega_0 = 0.4096$ [MHz]), the MSE of b_2 is the same as that of the CRLB, while the MSEs of b_1 and b_0 are about 3 and 7 [dB] above the MSEs of their CRLBs.

In the forth simulation we compared the MSE on estimating b_p of the proposed method with the instantaneous frequency rate (IFR) method [3, p. 386]. The IFR method in [3] was suggested for a single sensor. Therefore, we first estimated the DOA of the signal according to (20). We then defined the signal $\mathbf{y}(n) = \mathbf{a}^H(\hat{\theta}_i)\mathbf{x}(n)$ and used the IFR method to estimate $\mathbf{b}$ from $\{\mathbf{y}(n)\}_{n=n_0}^{n_0+N-1}$. We consider the same quadratic frequency modulated signal used in the simulation results in [3, Sec. IV, p. 389] with the parameters $\alpha = 1$, $b_0 = 1$, $b_1 = \pi/8$, $b_2 = 0.005$, $b_3 = 0.0001$, $n_0 = -(N-1)/2$, and $N = 515$. We used 1000 MC independent trials. The SNR used here

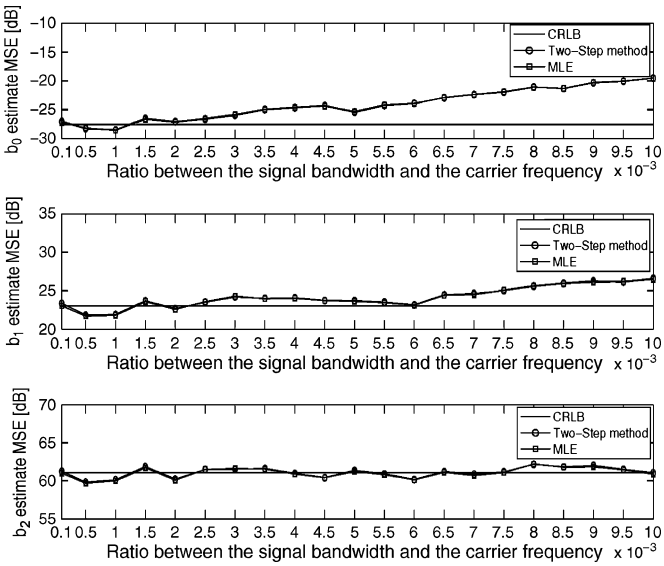

Fig. 3. MSEs of the estimated $\{b_p\}_{p=0}^{2}$ using the proposed method and the MLE, and their associated CRLBs, versus the ratio between the signal bandwidth and the carrier frequency.

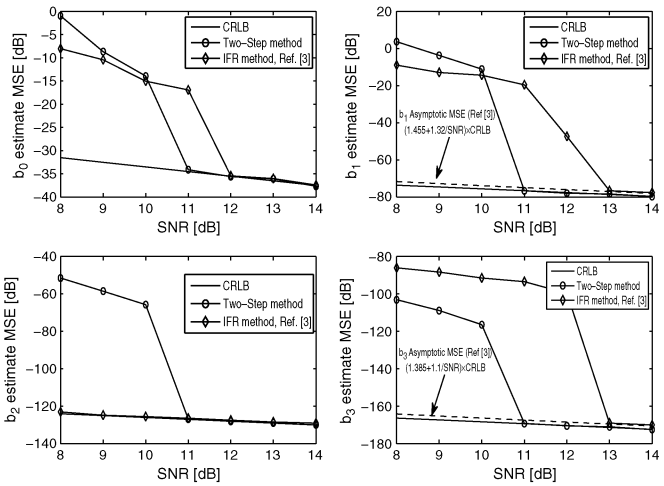

Fig. 4. MSEs of the estimated $\{b_p\}_{p=0}^{3}$ with the proposed method and the IFR method [3].

is identical to the definition in [3, following (39), p. 391]. The results are shown in Fig. 4. As a comparison, the CRLB is also plotted. The results of the MLE are omitted due to its high complexity in this case. In the two right plots, the asymptotic MSE of b_1 and b_3 is also plotted [3, Table I, p. 387]. The asymptotic MSEs of b_0 and b_2 were not added to the left plots since they coincide with the CRLB. As can be seen, and also mentioned in [3], the estimation of b_0 and b_2 converges to the CRLB, while the estimate of b_1 and b_3 is 38.5% and 45.5% above the CRLB. Notice that the MSEs of the proposed method converge to the CRLB. Only the MSE of b_2, using the IFR (related to the frequency rate), is better than that of the proposed method.

VII. Conclusions

In this paper, an efficient method to estimate the parameters of a polynomial phase signal observed by a sensor array was proposed. The method applies the ideas of the extended invariance property. Whereas the direct maximum likelihood method involves extensive complexity, the proposed algorithm only requires a simple one-dimensional search in the direction of arrival space. Monte Carlo simulations show that the estimated parameters converge to the Cramér–Rao lower bound at high signal-to-noise ratio.

Acknowledgment

The author wish to thank the three anonymous reviewers and the Associate Editor for their insightful and constructive comments, which helped to improve and clarify this paper.

References

[1] S. Peleg and B. Porat, "Estimation and classification of polynomial-phase signals," *IEEE Trans. Inf. Theory*, vol. 37, pp. 422–430, Mar. 1991.

[2] P. M. Djuric and S. M. Kay, "Parameter estimation of chirp signals," *IEEE Trans. Acoust., Speech, Signal Process.*, vol. 38, pp. 2118–2126, Dec. 1990.

[3] P. OShea, "A fast algorithm for estimating the parameters of a quadratic FM signal," *IEEE Trans. Signal Process.*, vol. 52, no. 22, pp. 385–392, Feb. 2004.

[4] P. Wang, I. Djurovic, and J. Yang, "Generalized high-order phase function for parameter estimation of polynomial phase signal," *IEEE Trans. Signal Process.*, vol. 56, pp. 3023–3028, Jul. 2008.

[5] B. J. Slocumb and J. Kitchen, "A polynomial phase parameter estimation-phase unwrapping algorithm," in *Proc. IEEE Int. Conf. Acoust., Speech, Signal Process. (ICASSP'94)*, Adelaide, Australia, Apr. 1994, vol. 4, pp. 129–132.

[6] A. Gershman, M. Pesavento, and M. G. Amin, "Estimating parameters of multiple wideband polynomial phase sources in sensor arrays," *IEEE Trans. Signal Process.*, vol. 49, pp. 2924–2934, Dec. 2001.

[7] M. Adjrad and A. Belouchrani, "Estimation of multicomponent polynomial phase signals impinging on a multisensor array using state-space modeling," *IEEE Trans. Signal Process.*, vol. 55, pp. 32–45, Jan. 2007.

[8] A. Zeira and B. Friedlander, "Direction of arrival estimation using parametric signal models," *IEEE Trans. Signal Process.*, vol. 44, pp. 339–350, Feb. 1996.

[9] A. Belouchrani and M. Amin, "Time-frequency MUSIC," *IEEE Signal Process. Lett.*, vol. 6, pp. 109–110, May 1999.

[10] A. Zeira and B. Friedlander, "On blind signal copy for polynomial phase signals," in *Proc. IEEE Int. Conf. Acoust., Speech, Signal Process. (ICASSP'97)*, Munich, Germany, Apr. 1997, vol. 5, pp. 4045–4048.

[11] S. Stoica and S. Soderstrom, "On reparameterization of loss functions used in estimation and the invariance property," *Signal Process.*, vol. 17, pp. 383–387, Aug. 1989.

[12] A. Leshem and A.-J. van der Veen, "Direction of arrival estimation for constant modulus signals," *IEEE Trans. Signal Process.*, vol. 47, pp. 3125–3129, Nov. 1999.

[13] H. L. Van Trees, *Detection, Estimation, and Modulation Theory: Optimum Array Processing—Part IV*. New York: Wiley, 2002.